Yanbu Journal of Engineering and Science

Volume 22 | Issue 1 Article 4

2025

Morphology and Properties of Hollow Fiber Membrane Prepared Under Different Air Gap Lengths

Aida Isma M.I.
Faculty of Engineering, Built Environment and Information Technology, Segi University, 47810 Kota Damansara, Selangor Darul Ehsan, Malaysia, aidaisma@segi.edu.my

Syeda Hina Iqbal
Faculty of Engineering, Built Environment and Information Technology, Segi University, 47810 Kota Damansara, Selangor Darul Ehsan, Malaysia

Omar R.
Department of Chemical and Environmental Engineering, Faculty of Engineering, Universiti Putra Malaysia, 43400 Serdang, Selangor Darul Ehsan, Malaysia

Hazmin M.
Department of Civil Engineering, Faculty of Engineering and Life Sciences, Universiti Selangor, 45600 Bestari Jaya, Selangor Darul Ehsan, Malaysia

Follow this and additional works at: https://yjes.researchcommons.org/yjes

The journal in which this article appears is hosted on Digital Commons, an Elsevier platform.

Recommended Citation

M.I., Aida Isma; Iqbal, Syeda Hina; R., Omar; and M., Hazmin (2025), Morphology and Properties of Hollow Fiber Membrane Prepared Under Different Air Gap Lengths, *Yanbu Journal of Engineering and Science*: Vol. 22: Iss. 1, 51-58.
DOI: https://doi.org/10.53370/001c.126170
Available at: https://yjes.researchcommons.org/yjes/vol22/iss1/4

This Research Article is brought to you for free and open access by Yanbu Journal of Engineering and Science. It has been accepted for inclusion in Yanbu Journal of Engineering and Science by an authorized editor of Yanbu Journal of Engineering and Science.

YANBU JOURNAL OF ENGINEERING AND SCIENCE 2025;22:51–58

Scan the QR to view the full-text article on the journal website

RESEARCH ARTICLE

Morphology and Properties of Hollow Fiber Membrane Prepared Under Different Air Gap Lengths

Aida Isma M.I. [a,*], **Syeda Hina Iqbal** [a], **Omar R.** [b], **Hazmin M.** [c]

[a] Faculty of Engineering, Built Environment and Information Technology, Segi University, 47810 Kota Damansara, Selangor Darul Ehsan, Malaysia
[b] Department of Chemical and Environmental Engineering, Faculty of Engineering, Universiti Putra Malaysia, 43400 Serdang, Selangor Darul Ehsan, Malaysia
[c] Department of Civil Engineering, Faculty of Engineering and Life Sciences, Universiti Selangor, 45600 Bestari Jaya, Selangor Darul Ehsan, Malaysia

ABSTRACT

The fabrication of hollow fibre membrane modules is affected by many spinning variables, including polymer composition, bath temperature, bore fluid ratio, fibre take-up velocity, and air gap length, resulting in varying properties. This study uses a dry-jet wet-spinning process to investigate the morphology and characteristics of PVDF hollow fibre membranes prepared at 10 cm (P10) and 20 cm (P20) air gap lengths. Polypropylene glycol was used as an additive. The dope extrusion rate, coagulation bath temperature, bore fluid ratio, and take-up velocity were set at 4 rpm, 30°C, 1.5 ml/hr, and 2 m/min, respectively. Atomic force microscopy determined the pore size distribution, roughness, and membrane thickness. Field emission scanning electron microscope (FESEM) analyzed membrane morphology. Membrane performance was tested using 10 mg/L of synthetic protein solution. The results showed that the diameters of the fibers as well as the inner and outer lumens were significantly influenced by the air gap. Membrane dimensions decreased with the increased air gap distance with the outer and inner diameter by 5% at a 10 cm air gap. FESEM images verified that the thickness of the skin layer increases with the increase in air gap distance. The resulting roughness of the membrane layer was found to be dependent on the pore size of the support layer. The protein separation test achieved the best rejection of 98% using the P20 membrane. Thus, selecting an optimum air gap distance for hollow fibre membrane fabrication was discovered to be a viable strategy for improving separation performance in membrane filtration and improving solute separation in wastewater.

Keywords: Air gap length, Flux, Hollow fibre membrane, Surface roughness

1. Introduction

Membrane technology has become the most convincing water treatment process due to its numerous benefits, including its simplicity of operation, low carbon footprint and energy usage with high-efficiency treatment [1–4]. Nonetheless, exploring desirable membranes is still an emerging field for membrane separation processes.

Many studies highlight advances in optimising polyvinylidene fluoride (PVDF) hollow fibre membrane fabrication for environmental sustainability and efficiency. Zakria et al. used less toxic solvents [5], Suzana et al. developed membranes for dye/salt separation [6] and Hamed et al. prepared PVDF-co-CTFE for harsh alkaline conditions [7]. Isabel et al. recommended further research on the sustainability

Received 12 March 2024; revised 19 September 2024; accepted 27 October 2024.
Available online 1 June 2025

* Corresponding author.
E-mail address: aidaisma@segi.edu.my (Aida Isma M.I.).

https://doi.org/10.53370/001c.126170
1658-5321/© 2025 The Author(s). Yanbu Journal of Engineering and Science. This is an open access article under the CC BY 4.0 Licence (https://creativecommons.org/licenses/by/4.0/).
Published by Yanbu Industrial College, Saudi Arabia. The journal is hosted on Digital Commons, an Elsevier Platform.

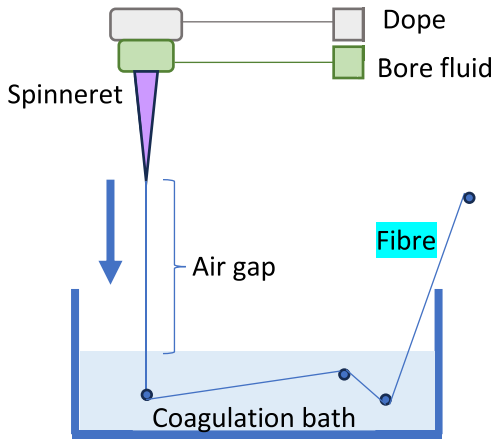

Fig. 1. Dry-jet wet spinning process to form hollow fibre membranes.

of green manufacturing components and their integration into membranes [8].

Fabrication of affordable membranes with high selectivity and permeability and acceptable thermal stability and mechanical properties is challenging. Spinning variables during hollow fibre fabrication are crucial in determining the physical properties of the membrane. The factors include the coagulant bath temperature, the amount and type of polymers and solvents, the composition of the dope solution, the dope rate, the fibre take-up velocity, the bore fluid used, and the air gap distance [9, 10]. The kinetics of phase inversion, which significantly impacts the ultimate form of a membrane, can be affected by several factors during the production of hollow fibre membranes. Additionally, inducing non-solvent additives will increase the viscosity of the dope solution, reducing the solvent diffusion and the non-solvent in the external bath [11].

Due to their advantages, hollow fibre membranes have become popular compared to flat sheet membranes, as they have a large surface area per unit volume, high density, and a high degree of flexibility during operation [12]. The early studies employed on hollow fibre fabrication include design and membrane modules [13], the preparation methods of polyvinylidene fluoride membrane [14], surface alteration [15], the effect of additives [16] and the effect of air gap length for gas absorption [17].

PVDF membranes can be used to produce fresh water from seawater and address water shortages in coastal regions [18]. The tunable properties of PVDF membranes make them suitable for large-scale industrial desalination and water treatment projects [19].

Fig. 1 shows the vertical space between the spinneret and the liquid coagulation bath, known as the air gap, a crucial characteristic in changing the membrane's outer layer that should be explored and controlled during membrane fabrication. The dope extrusion flow rate will determine the hollow fibre thickness after precipitation, and the coagulation bath will complete the phase inversion of the external layer of hollow fibres. The polymer solution is extruded through the spinneret during the spinning process and solidifies into a membrane through a phase inversion process. This study uses a dry-jet wet-spinning approach to investigate the morphology membranes prepared at different air gap distances of 10 cm and 20 cm, respectively.

2. Materials and methods

2.1. Materials

The PVDF (Hylar® 301S) used as the main material was first dried at 60°C. The solvents dimethylacetamide (DMAC) (anhydrous 99.8%, Merck) and isopropyl alcohol (ACS < 100%, Merck) were used for the polymer solution and wetting solutions, respectively. In contrast, ethylene glycol (AnalaR, 99.5%) was used as a non-solvent additive. Other materials, including 1-propanol, glycerol, and 1-methyl-cyclohexanol, were used to make polypropylene glycol (PG), a self-made additive of analytical reagent.

2.2. Membrane fabrication

PVDF is widely used as a membrane material due to its high thermal stability, mechanical strength, hydrophobicity, and chemical resistance [20]. Aprotic solvents, like NMP, DMSO, DMF and DMAC dissolve PVDF, enabling membrane fabrication through phase separation methods. PVDF/DMAC/PG were maintained at a weight ratio of 16/62/22. Using a magnetic stirrer, PG was dissolved in DMAC for 30 min at 60°C and 600 rpm. PVDF was added to the mixture and stirred for another 6 hours. The dope solution was immersed in an ultrasonicated bath for 15 min for degassing purposes. After that, the dope solution was ready for hollow fibre spinning.

The synthesis dope solutions were spun at two distinct air gap distances, 10 cm and 20 cm, respectively, denoted as P10 and P20. Dry jet-wet spinning was used to spin the fibre following Ismail et al. [21]. Other spinning parameters were kept constant. The minimum take-up drum speed was maintained at 0.033 m/s manually, which allowed the fibres to be stretched gravitationally while avoiding coagulation bath accumulation.

All spinning parameters were kept constant throughout the process. Room temperature water

was used for the bore fluid and coagulation bath. The drum extrusion and bore fluid rates were tuned at 4 rpm and 0.025 ml/min, respectively. The membranes were submerged in water for 48 hours to eliminate solvent traces, followed by submerging in a glycerol/water mixture (50 v/v%) for another 24 hours before being dried at room temperature to retain the membrane pore structure.

2.3. Membrane morphology

The cross-sectional structure, shape and dimensions of the membranes and fibres were monitored using field emission scanning electron microscopy (FESEM, JEOL Model JSM-7800F). The fibres were coated with a thin coating of gold film using a sputter coater before the characterization. The membrane cross-section was fractured using liquid nitrogen. The membrane diameters were measured using an image analyzer. Atomic forced microscopy (AFM) was used to examine the mean roughness (Ra) and nodule size of the outer surface of hollow fibre membranes. The images were captured using AFM equipment (SPA 300HV, Japan) over a scan area of 4 μm $\times$ 4 μm.

2.4. Flux and rejection performance

The prepared membrane modules were subjected to hydraulic compression using deionized water as feed for 30 min before the flux performance test. The membrane modules were then subjected to 60 min water flux test. The flux was determined using the following equation:

$$J = \frac{Q}{At} = \frac{Q}{n\pi dt} \quad (1)$$

where J (L/m^2.h) is the flux, Q (L) is the total filtrate, n is the number of fibres, d (m) is the inner diameter, and t (h) is the permeation time. To evaluate the rejection performance, a feed solution of 10 mg/L bovine serum albumin (BSA) in deionized water (pH 7.0 adjusted with 0.1 M NaOH solution) was introduced for 60 min at the same flow rate. The permeate sample was used to determine bovine serum albumin (BSA) using HACH spectrophotometer at 280 nm. The rejections were calculated using the following:

$$\text{Rejection, R} = \frac{C_o - C}{C_o} \times 100 \quad (2)$$

where R (%) is the BSA rejection, C_o (mg/L) is the BSA concentration of permeate, and C (mg/L) is the BSA concentration of the feed.

3. Results and discussions

3.1. Cross-sectional morphology

A higher air gap led to a longer residence time for hollow fibre in the air, which led to a thicker skin layer [22]. The length of the air gap restraints the time the fibre is exposed to air during spinning. The spinning air gap length of the PVDF hollow fibre membrane resulted in different membrane morphologies as shown in Fig. 2. Fig. 2(a) demonstrates a non-circular lumen generated at a 10 cm air gap (P10), while a circular lumen was formed at a 20 cm air gap (P20). The overall cross-section of the hollow fibre membranes showed that the fibre did not have sufficient time to relax and lessen the effect of die swelling, caused by the small air gap. With an increase in air gap distance, the membrane dimensions shrank, with the outer diameter (OD) shrank from 649 to 619 nm at a 10 cm air gap, while the inner lumen diameter (ID) shrank from 530 nm to 499 nm. The outer and inner diameters of the hollow fibre sample spun at 20 cm were reduced by 5% and 6%, respectively, from the initial values of 649 nm and 530 nm.

During the phase inversion process used in PVDF membrane fabrication, factors like solvent concentration, non-solvent type, and coagulation bath temperature determine the rate of phase separation. Faster phase separation leads to larger pores, while slower separation yields a denser structure with smaller pores, impacting both permeability and rejection [23]. The hollow fibre elongation mainly drove the significant decrease in OD and ID due to gravity as it passed through the air gap [24]. When water was used as the bore fluid, the internal surface precipitated instantly, causing internal build-up in the nascent fibre as the die swelling effect faded. The lumen was squeezed, leading to non-circularity. Furthermore, the results are similar to those previously reported for other polymeric membranes, such as PES/PVA [25]. Similar findings were reported by Korminouri et al., [26], who discovered a decrease in inner diameter from 493 to 415 μm and a reduction in outer diameter from 837 to 780 μm, with an increase in air gap. The decrease was attributable to gravity-induced elongation of the hollow fibre membrane at more significant air gaps.

Fig. 2(b) shows the FESEM images of the internal surface of the spun membrane at 20,000 magnifications. Pore size and wall thickness decreased by 45% from 0.365 to 0.2 μm and 5% from 61.1 to 57.9 nm for P10 and P20 membranes, respectively. All membrane surfaces had identical pores formation throughout the length of the membranes, implying that the

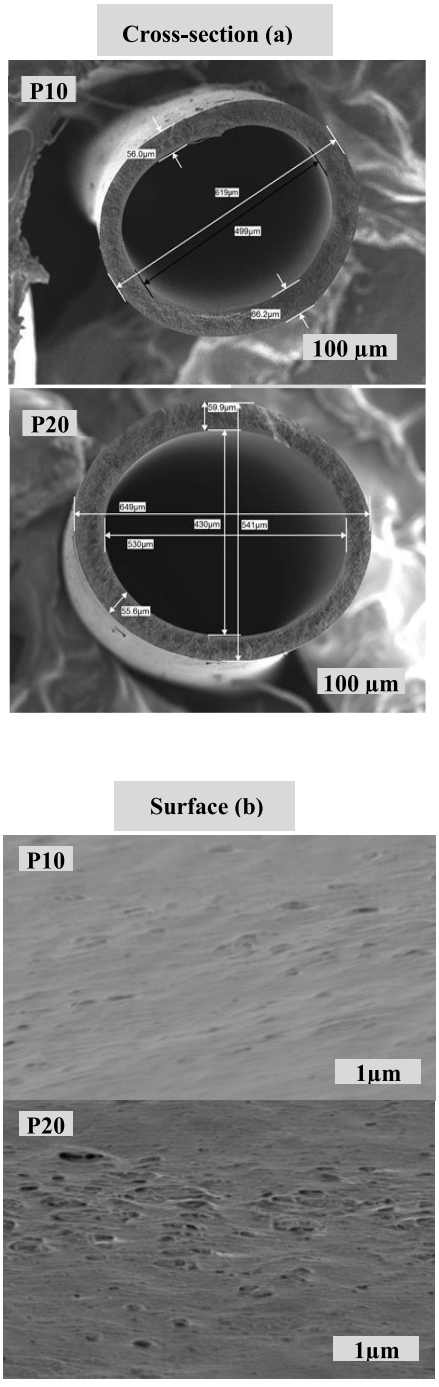

Fig. 2. (a) FESEM cross-sectional and (b) surface micrograph of hollow fibre membrane.

morphology was caused by gravitational stretching. Longer evaporation times may have made more pores visible at longer air gaps. As a result, before the outer surface of the fibre reaches the external coagulation bath, it suffers phase separation caused by volatile solvent evaporation and stress-induced orientation. Additionally, the type of external coagulant (weak or strong) used influences the formation of pores.

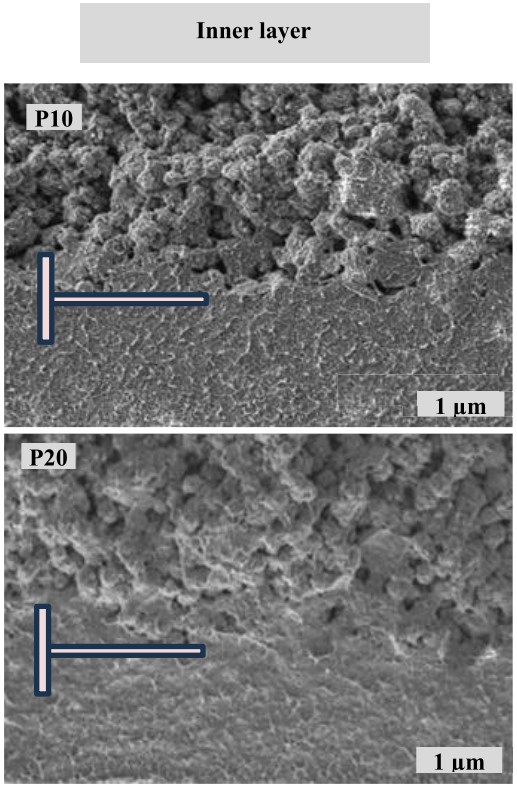

Fig. 3. Inner layer of external section of hollow fibre membrane (at x5000 magnification).

Previous research has shown that the most favourable molecular orientation of the polymer, which enhances polymer chain packing, requires an optimal evaporation duration during dry/wet spinning [27].

Figs. 3 and 4 show the inner and outer layers, respectively, of the external section of the spun membrane. The outer part shows more of a microporous formation, whereas no porous structures on the inner part for both membranes. The porous skin layer for all membranes emerges from the outer and inner surfaces of hollow fibres and stretches to the central part of the fibre.

The hollow fibre, at the lower air gap (P10), exhibited a sandwich-like structure, and at a higher air gap (P20), the membranes showed an asymmetrical arrangement of finger-like along with macro-voids and a compact sponge-like sublayer. Furthermore, the micro void finger-like shape altered to a sponge-like structure. With the extended contact time between the spun fibre and the inner coagulant (water), the size of micro-voids grows as the air gap widens [28]. Hollow fibre spun with longer air gaps has tighter molecular packing and more excellent molecular orientation [29].

Shao et al., [30] found that increasing the air-gap in PVDF membranes led to a more pronounced

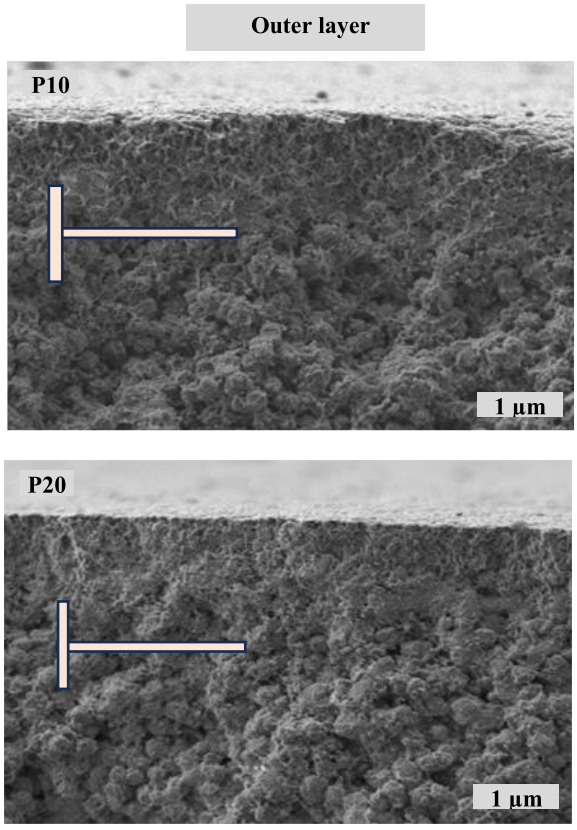

Fig. 4. Outer layer of external section of hollow fibre membrane (at x5000 magnification).

sponge-like structure with larger voids and reduced mechanical strength. Similarly, Li et al., [31] reported that a larger air gap in polysulfone membranes produced a sponge-like sublayer with enhanced flux but decreased mechanical strength. Wang et al., [32] observed that higher air gaps in PVDF hollow fiber membranes resulted in sponge-like sublayers, increasing flux but compromising stability. Zhang et al., [33] demonstrated that in membrane distillation modules, a greater air gap formed sponge-like structures with improved thermal insulation but weakened mechanical properties.

3.2. AFM observation

Gravity influences the formation of membrane morphology significantly while nascent fibre flows in the air gap. Matveev et al. [34] analyzed how air gap length and gravity contribute to the elongation and thinning of fibres, altering pore structure and ultimately affecting membrane permeability and rejection. AFM is employed to evaluate the surface roughness of the membranes. Fig. 5 displays the AFM micrographs of the outer surface of hollow fibres spun at air gap lengths of 10 cm (P10) and 20 cm (P20).

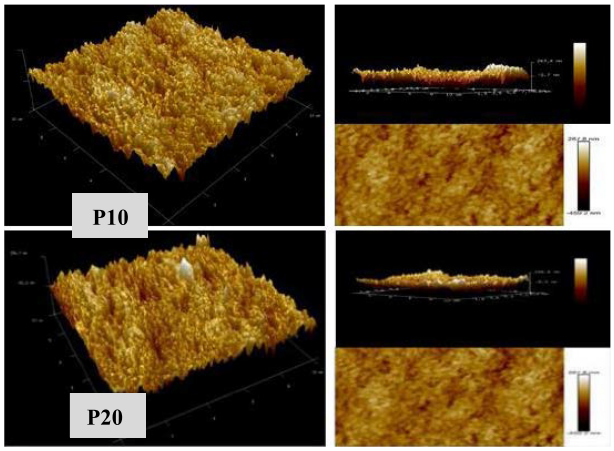

Fig. 5. AFM surface topography of membrane at different air gap lengths.

Table 1. Surface roughness values of P10 and P20.

Membrane	R_a	R_{max}	RMS (nm)	Nodule
P10	60.3 ± 0.28	550 ± 0.33	60.3 ± 2.97	59 ± 0.76
P20	48.6 ± 0.27	545 ± 0.64	48.6 ± 2.23	71 ± 0.52

A longer air gap results in a more homogenous pore formation.

The agglomeration occurrences were absent on the surface of the membrane, indicating homogenous blending of the dope solution. However, an uneven surface was also evident from the image distributed across the top membrane, with the dark region characterized as pores and the bright regions seen as nodules. An increase in air gap can lead to delayed phase inversion resulting in the formation of finger-like structures, a decrease in the macro-void size, and a reduction in permeance [35].

Table 1 showed surface roughness characteristics determined as mean roughness (RMS), mean square of the Z data (Ra), and mean difference of the five highest peaks (R_{max}). Results show that the P10 membrane had a roughness that was noticeably higher than the P20 membrane at 60.3 nm and 48.6 nm, respectively.

All membrane nodule structures had an agglomeration distribution that frequently influences membrane performance. Studies show that as surface roughness rises, flow and permeability increase [36]. It can be concluded that as the air gap expanded, the roughness values decreased, and the nodule size increased.

3.3. Pure water permeability and rejection performance

Table 2 shows the experimental results for water flux and BSA rejection during the one-hour

Table 2. Flux and rejection performance.

Membrane sample	Water flux (LMH)	Rejection (%)
P10	1.5 ± 0.84	94.9
P20	1.7 ±	98.9

permeation test; both membranes showed stable fluxes. Variations in separation performance will result from changes in membrane structure. The porosity, pore size and pore distribution of PVDF membranes significantly influence permeability. Membranes with larger pores and higher porosity allow more water to pass through, resulting in higher permeability. Conversely, smaller pore sizes or denser structures impede water flow, reducing permeability. The rejection of BSA by the P20 membrane sample was the highest at 98.9%, with P10 membrane sample rejection dropping to 4%. The pore size also directly affects rejection. Membranes with smaller pore sizes provide better rejection of solutes, as smaller molecules or particles are more easily filtered out. Larger pores may allow more contaminants or solutes to pass through, reducing rejection efficiency. The formulation of the membranes was the same, suggesting similar surface chemistry. Hence, the rejection trend was solely due to the difference in pore size.

4. Conclusion

The effect of air gap distances on the morphology and performance of membranes was investigated. The outer and inner membrane diameters were reduced with increasing air gap. FESEM verified that the thickness of the skin layer increases with the increase in air gap distance from 10 cm to 20 cm, as anticipated with the excellent molecular orientation. The resulting roughness of the membrane layer was found to be dependent on the pore size of the support layer. The air gap of the P20 membrane shows high water flux which is due to the thickness of the support layer, porosity, and pore structure. Hence, establishing a smooth and stable spinning line requires careful tuning and adjustment of the air gap distance.

Acknowledgements

The authors gratefully thank and acknowledge the financial support from SEGi University.

Abbreviation

AFM	Atomic forced microscopy
BSA	bovine serum albumin
C	concentration of feed
C_o	concentration of permeate
FESEM	Field emission scanning electron microscope
J	flux
LMH	$L/m^2.h$
P_{10}	10 cm air gap
P_{20}	20 cm air gap
PVDF	polyvinylidene flouride
Q	flowrate
R	rejection
R_a	mean square of the Z data
R_{max}	mean difference of the highest peaks
RMS	mean roughness

Conflict of interest

The authors declare no conflict of interest.

Author contribution

Aida Isma M.I. was responsible for writing the manuscript, visualization, software analysis, revision and finalization of the manuscript.

Syeda Hina Iqbal did the experimentation, participated in the analysis and reviewed the manuscript. Omar R. did the microscopy, software analysis and revision of the manuscript. Hazmin M. testing, software analysis and revision of the manuscript.

Data availability

The authors confirm that the data supporting the findings of this study are available within the article [and/or] its supplementary materials.

References

1. Huang Y, Xiao C, Huang Q, Liu H, Zhao J. Progress on polymeric hollow fiber membrane preparation technique from the perspective of green and sustainable development. Chem. Eng. J. 2021;403:126295. https://doi.org/10.1016/j.cej.2020.126295.
2. Tanaka Y, Yasukawa M, Goda S, Sakurai H, Shibuya M, Takahashi T, Kishimoto M, Higa M, Matsuyama H. Experimental and simulation studies of two types of 5-inch scale hollow fiber membrane modules for pressure-retarded osmosis. Desalination. 2018;447:133–146. https://doi.org/10.1016/j.desal.2018.09.015.
3. Wang X, Zhang L, Yang H, Chen H. Feasibility research of potable water production via solar-heated hollow fiber membrane distillation system. Desalination. 2009;247:403–411. https://doi.org/10.1016/j.desal.2008.10.008.
4. Zhang Z, Ning K, Xu Z, Zheng Q, Tan J, Liu Z, Wu Z, Zhang G, Jin W. Highly efficient preparation of Ce0.8Sm0.2O2-δ– SrCo0.9Nb0.1O3-δ dual-phase four-channel hollow fiber

membrane via one-step thermal processing approach. J. Memb. Sci. 2021;620:118752. https://doi.org/10.1016/j.memsci.2020.118752.
5. Zakria HS, Othman MHD, Kadir SHSA, Kamaludin R, Jilani A, Omar MF, Bakar SA, Jaafar J, Rahman MA, Abdullah H et al. Fabrication of High Performance PVDF Hollow Fiber Membrane Using Less Toxic Solvent at Different Additive Loading and Air Gap. Membranes 2021;11:843. https://doi.org/10.3390/membranes11110843.
6. Syed UT, Upadhyaya L, Loiola LMD, Emwas A-H, Volkov A, Nunes SP. Thymol: nature's solvent for sustainable hollow fiber fabrication. Green Chem. 2024. https://doi.org/10.1039/D4GC01961J.
7. Karkhanechi H, Vaselbehagh M, Jeon S, Shaikh AR, Wang Da-, Matsuyama H. Preparation and characterization of polyvinylidenedifluoride-co-chlorotrifluoroethylene hollow fiber membranes with high alkaline resistance. Polymer. 2018;145:310–323, ISSN 0032-3861. https://doi.org/10.1016/j.polymer.2018.04.074.
8. Dong X, Lu D, Harris TAL, Escobar IC. Polymers and Solvents Used in Membrane Fabrication: A Review Focusing on Sustainable Membrane Development. Membranes. 2021;11(5):309. doi: 10.3390/membranes11050309.
9. Feng CY, Khulbe KC, Matsuura T, Ismail AF. Recent progresses in polymeric hollow fiber membrane preparation, characterization and applications. Sep. Purif. Technol. 2013;111;43–71. https://doi.org/10.1016/j.seppur.2013.03.017.
10. Wang D, Li K, Teo WK. Preparation and characterization of polyvinylidene fluoride (PVDF) hollow fiber membranes. Journal of Membrane Science. 1999;163(2):211–220. https://doi.org/10.1016/S0376-7388(99)00181-7.
11. Giwa A, Chakraborty S, Mavukkandy MO, Arafat HA, Hasan SW. Nanoporous hollow fiber polyethersulfone membranes for the removal of residual contaminants from treated wastewater effluent: Functional and molecular implications. Separation and Purification Technology. 2017;189:20–31. http://dx.doi.org/10.1016/j.seppur.2017.07.058
12. Khayet M. The effects of air gap length on the internal and external morphology of hollow fiber membranes. Chemical Engineering Science. 2003;58(14):3091–3104. https://doi.org/10.1016/S0009-2509(03)00186-6
13. Wan CF, Yang T, Lipscomb GG, Stookey DJ, Chung T-S. Design and fabrication of hollow fiber membrane modules.Journal of Membrane Science. 2017;538:96–107. https://doi.org/10.1016/j.memsci.2017.05.047
14. Kang GD, Cao YM. Application and modification of poly(vinylidene fluoride) (PVDF) membranes - A Review. J. Membr. Sci. 2014;463:145–165. https://doi.org/10.1016/j.memsci.2014.03.055
15. Wang X, Zhang Y, Liu Z. Effect of air gap on the morphology and filtration performance of PVDF hollow fiber membranes. Desalination. 2023;556:116256. https://doi.org/10.1016/j.seppur.2014.06.017
16. Li H-B, Shi W-Y, Zhang Y-F, Liu D-Q, Liu X-F. Effects of Additives on the Morphology and Performance of PPTA/PVDF in-situ Blend UF Membrane. Polymers. 2014;6:1846–1861. https://doi.org/10.3390/polym6061846
17. Kang G-D, Cao Yi-M. Application and modification of poly(vinylidene fluoride)(PVDF) membranes - A review. Journal of Membrane Science. 463;145–165.
18. Mohammad Amin Shahmirzadi A, Jalali K, Kargari A. Chapter 14 - Electrospun and nanofibrous membranes for membrane distillation, Editor(s): A Kargari, T Matsuura, Mohammad Mahdi A. Shirazi. Electrospun and Nanofibrous Membranes, Elsevier. 2023;371–407, ISBN 9780128230329. https://doi.org/10.1016/B978-0-12-823032-9.00005-2.
19. Shekari R, Dehban A, Kargari A. Fabrication of PVDF membranes via VIPS-NIPS technique for water desalination: Effect of preparation condition. Desalination and Water Treatment. 2024;319:100447, ISSN 1944-3986. https://doi.org/10.1016/j.dwt.2024.100447.
20. Kahrs C, Gühlstorf T, Jan Schwellenbach. Influences of different preparation variables on polymeric membrane formation via nonsolvent induced phase separation. Journal of Applied Polymer Science. 2019;137(28). https://doi.org/10.1002/app.48852.
21. Ismail AF, Shilton SJ, Dunkin IR, Gallivan SL. Direct measurement of rheologically induced molecular orientation in gas separation hollow fibre membranes and effects on selectivity. Journal of Membrane Science. 1997;126(1):133–137. doi:10.1016/s0376-7388(96)00274-8.
22. Rosid SM, Hasbullah H, Raharjo Y, Ismail AF, Othman MHD, Kadir SHSA, Kamal F, Abdullah MS, Ng BC. Effect of air gap distance of PSF/IONPs/ALG hollow fiber membrane on morphology and antifouling properties. Mater. Today Proc. 2021;46:1929–1933. https://doi.org/10.1016/j.matpr.2021.02.224
23. Pagliero M, Bottino A, Comite A, Costa C. Novel hydrophobic PVDF membranes prepared by nonsolvent induced phase separation for membrane distillation. Journal of Membrane Science. 2020;596:117575. https://doi.org/10.1016/j.memsci.2019.117575.
24. Abdul Latif Ahmad, Tunmise A Otitoju, Boon S Ooi. Hollow fiber (HF) membrane fabrication: A review on the effects of solution spinning conditions on morphology and performance. Journal of Industrial and Engineering Chemistry 2018. https://doi.org/10.1016/j.jiec.2018.10.005.
25. Ahmad AL, Mohd Shafie, ZMH. Effect of air gap distance on PES/PVA hollow fibre membrane's morphology and performance. J. Phys. Sci. 2017;28(Supp. 1):185–199. https://doi.org/10.21315/jps2017.28.s1.12.
26. Korminouri F, Rahbari-Sisakht M, Rana D, Matsuura T, Ismail AF. Study on the effect of air-gap length on properties and performance of surface modified PVDF hollow fiber membrane contactor for carbon dioxide absorption. Sep. Purif. Technol. 2014;132:601–609. https://doi.org/10.1016/j.seppur.2014.06.017.
27. Alexandr V Bildyukevich, Tatiana V Plisko, Alena S Liubimova, Vladimir V Volkov, Vadim V Ususky. Hydrophilization of polysulfone hollow fiber membranes via addition of polyvinylpyrrolidone to the bore fluid. Journal of Membrane Science. 2017;524:537–549, ISSN 0376-7388. https://doi.org/10.1016/j.memsci.2016.11.042.
28. Mohammadreza Kamali, Suhas DP, Maria Elisabete Costa, Isabel Capela, Tejraj M. Aminabhavi. Sustainability considerations in membrane-based technologies for industrial effluents treatment, Chemical Engineering Journal. 2019;368:474–494, ISSN 1385-8947. https://doi.org/10.1016/j.cej.2019.02.075.
29. Wang DK, Elma M, Motuzas J, Hou W-C, Xie F, Zhang X. Rational design and synthesis of molecular-sieving, photocatalytic, hollow fiber membranes for advanced water treatment applications. J. Memb.Sci. 2017;524:163–173. https://doi:10.1016/j.memsci.2016.10.052.
30. Shao M, Zhang H, Liu Y. Influence of air gap on the morphology and performance of PVDF membranes. Journal of Membrane Science. 2022;645:120011.

31. Li L, Chen Y, Zhao C. Air gap effects on the structure and performance of polysulfone ultrafiltration membranes. Separation and Purification Technology. 2021;263: 118315.
32. Wang X, Zhang Y, Liu Z. Effect of air gap on the morphology and filtration performance of PVDF hollow fiber membranes. Desalination. 2023;556:116256.
33. Zhang Q, Sun J, Zhang W. Optimization of air gap length for membrane distillation modules: Effects on membrane structure and performance. Journal of Membrane Science. 2022;655:120601.
34. Matveev DN, Anokhina TS, Volkov VV *et al.* Fabrication of Hollow Fiber Membranes: Effect of Process Parameters (Review). Membr. Membr. Technol. 2023;5(Suppl 1):S1–S21. https://doi.org/10.1134/S2517751623070016.
35. Dong X, Lu D, Harris TAL, Escobar IC. Polymers and Solvents Used in Membrane Fabrication: A Review Focusing on Sustainable Membrane Development. Membranes (Basel). 2021 Apr 23;11(5):309. doi: 10.3390/membranes11050309. PMID: 33922560; PMCID: PMC8146349. https://doi.10.3390/membranes11050309.
36. Huang Y, Xiao C, Huang Q, Liu H, Zhao J. Progress on polymeric hollow fiber membrane preparation technique from the perspective of green and sustainable development. Chemical Engineering Journal. 2021;403:126295, ISSN 1385-8947. https://doi.org/10.1016/j.cej.2020.126295.